



*The Abdus Salam  
International Centre for Theoretical Physics*



**2137-34**

**Joint ICTP-IAEA Advanced Workshop on Multi-Scale Modelling for  
Characterization and Basic Understanding of Radiation Damage  
Mechanisms in Materials**

*12 - 23 April 2010*

**SANS studies of microstructural radiation damage evolution in model alloys and  
technical steels for nuclear applications**

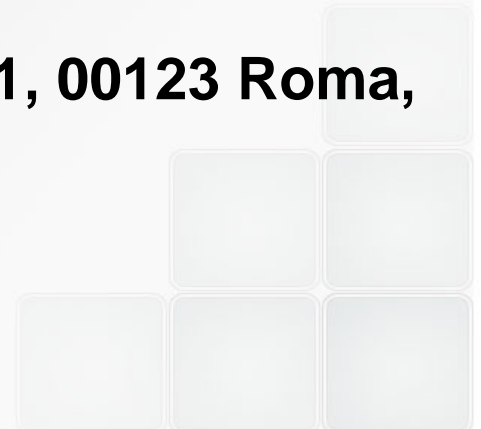
R. Coppola  
*ENEA-Casaccia  
Rome  
Italy*



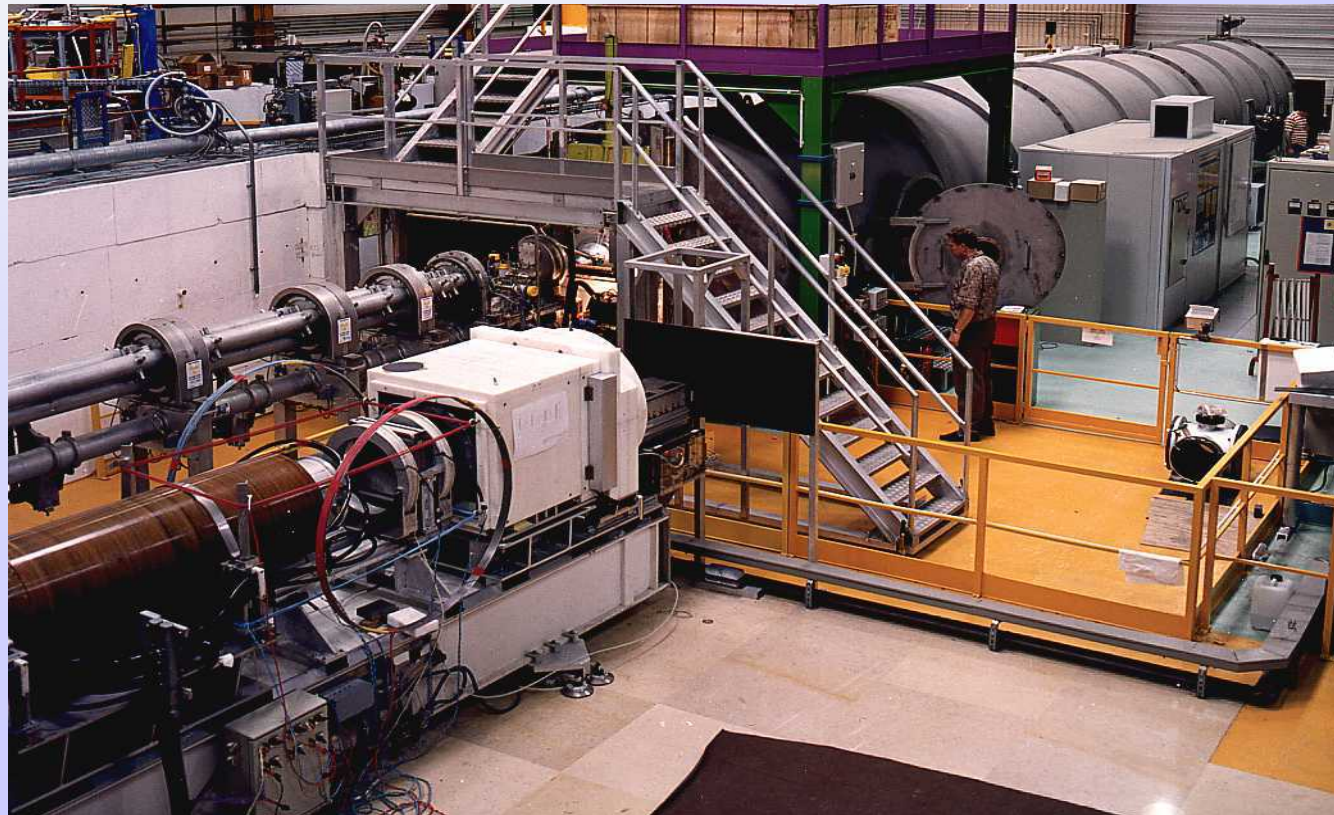
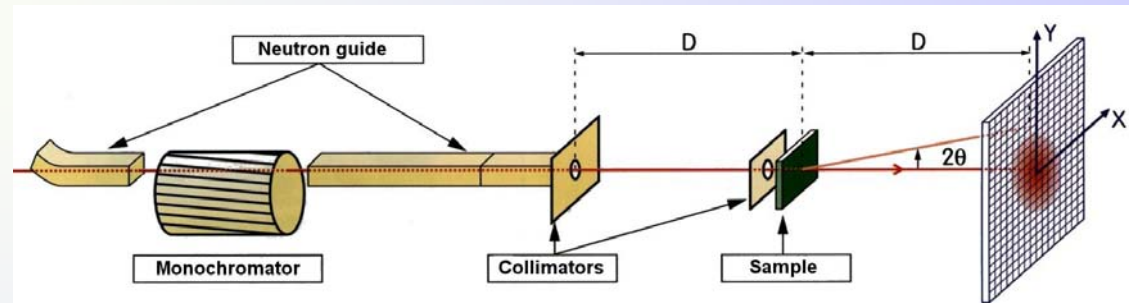
**SANS studies of microstructural radiation damage evolution in model alloys and technical steels for nuclear applications**

**Joint ICTP/IAEA Advanced Workshop on Multi-Scale Modelling**

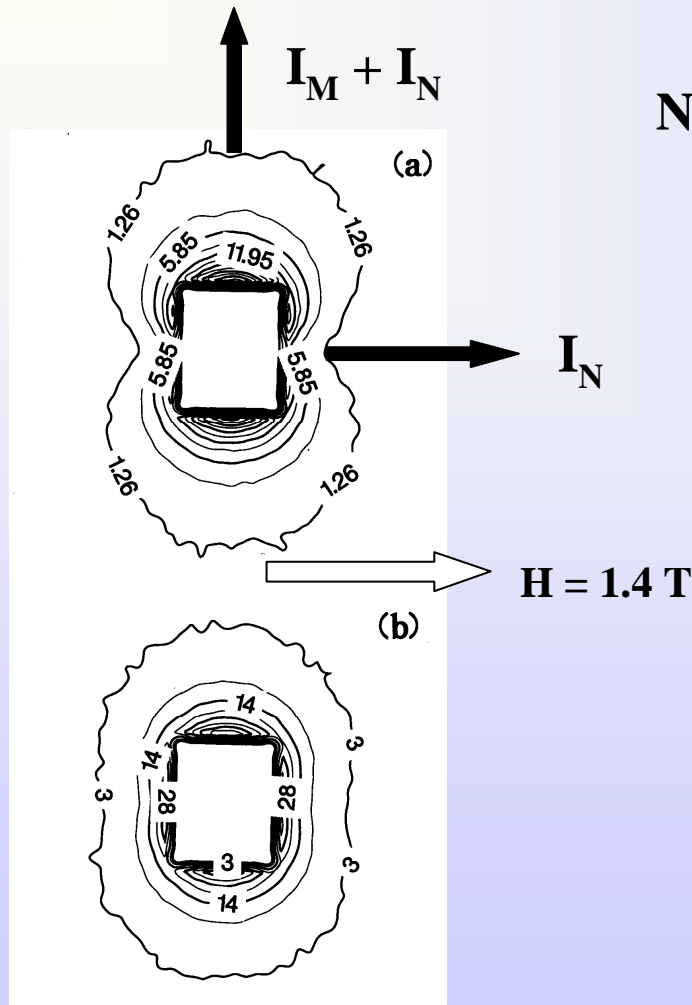
**R. Coppola, ENEA-Casaccia, Via Anguillarese 301, 00123 Roma, Italy**



# SANS INSTRUMENT D22 AT THE ILL-GRENOBLE



# NUCLEAR AND MAGNETIC SANS



## Nuclear and magnetic SANS cross-section

$$\frac{d\Sigma(Q)}{d\Omega} = (\Delta\rho)^2 \int_0^\infty dR N(R) V^2(R) |F(Q, R)|^2$$

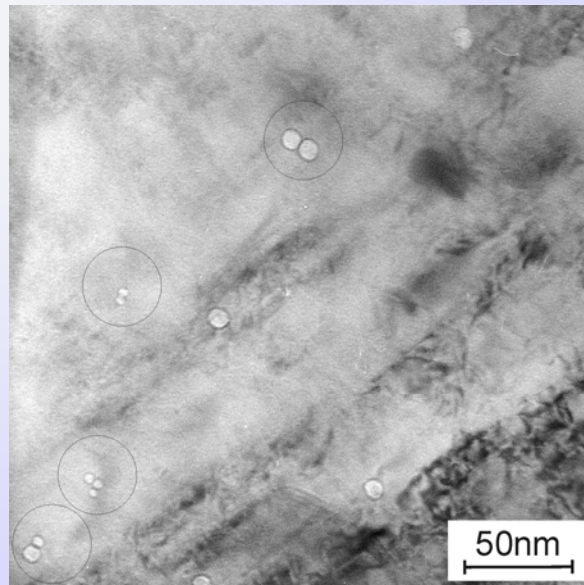
$$R(Q) = \frac{\frac{d\Sigma(Q)}{d\Omega_{nucl}} + \frac{d\Sigma(Q)}{d\Omega_{mag}}}{\frac{d\Sigma(Q)}{d\Omega_{nucl}}} = 1 + (\Delta\rho)_{mag}^2 / (\Delta\rho)_{nucl}^2$$

## Polarised SANS

$$A_M \cdot A_N \propto \Delta\rho_m \cdot \Delta\rho_n$$

a) reference sample, b) irradiated sample

**He bubbles in F82H-mod. steel implanted with  $\alpha$ -particles at RT then annealed 2 h at temperatures between 250° C and 975 °C**



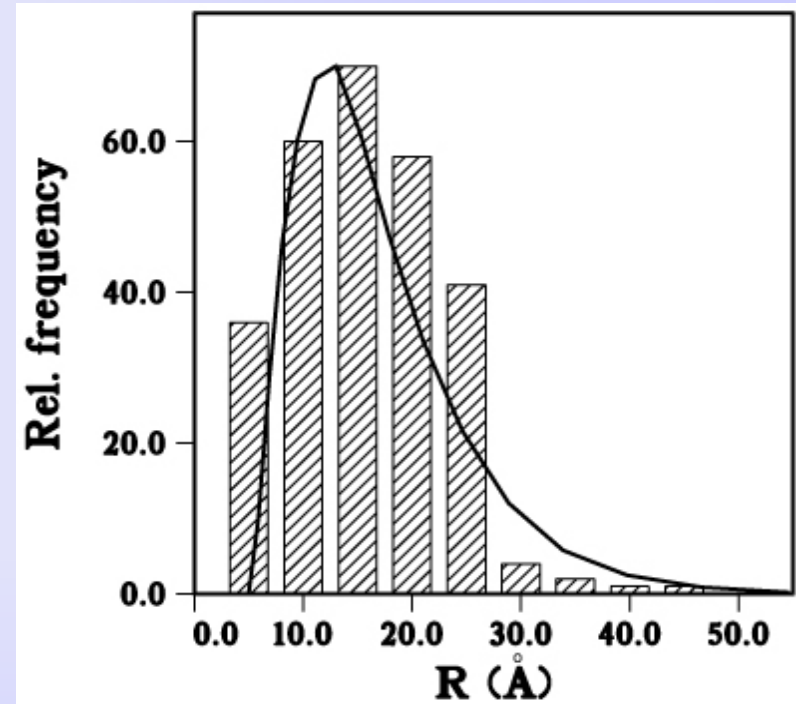
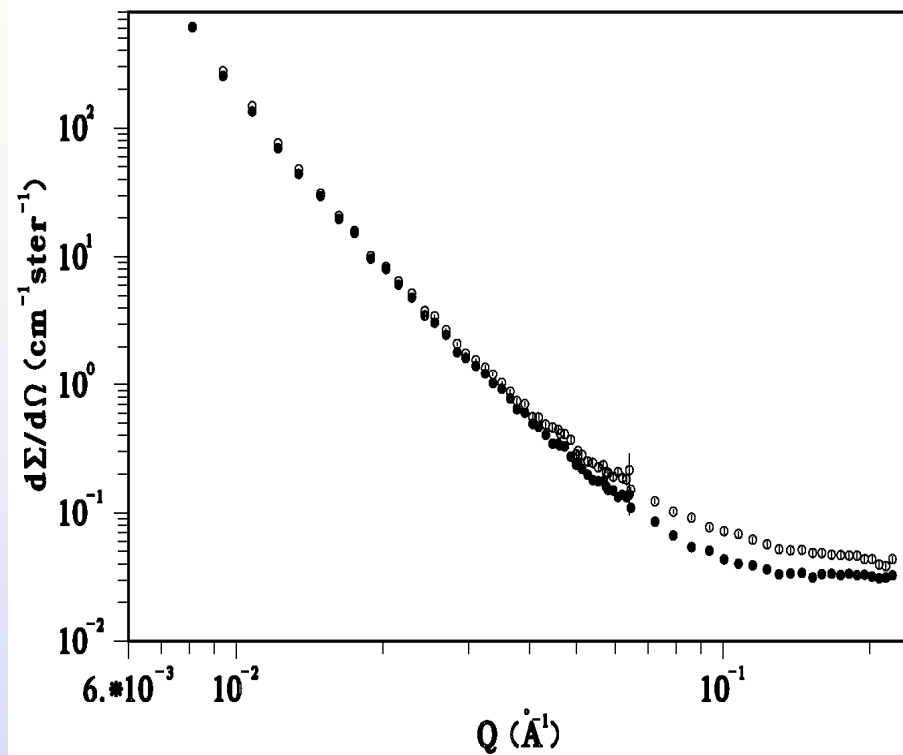
Coalescence of helium bubbles after annealing at 975 °C  
(M. Klimiankou, FZK)

## SANS contrast depends on bubble radius $R$

$$\Delta \rho (R) = \rho_{F82H} - b_{He} \rho_{He}(R)$$

$$C_{He} = v_M \int \rho_{He}(R) V(R) N(R) dR$$

The dependence of the contrast on the bubble radius is taken into account in the fitting procedure but given the small value of  $\rho_{He}$  very large changes of the He mass density would be necessary to lead to significantly different distributions. Assuming that the He concentration is equal to the nominal value (400 appm), the obtained variations on range typically from  $-10\%$  at  $2 \text{ \AA}$  to  $+12\%$  at  $100 \text{ \AA}$ . The resulting variations in  $N(R)$  are generally of a few per cent, therefore well inside the statistical uncertainty band

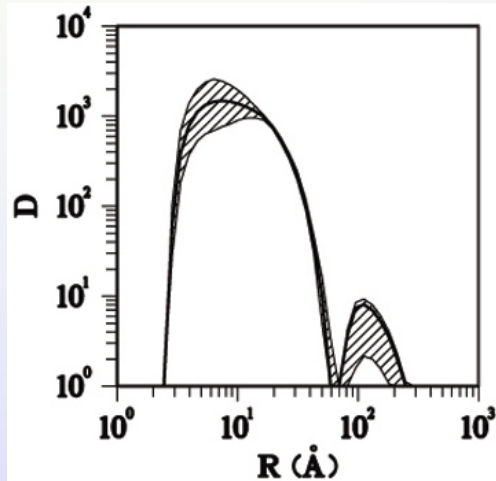


F82H-mod. steel as-implanted at  $250^\circ\text{C}$  then tempered at  $825^\circ\text{C}$ :

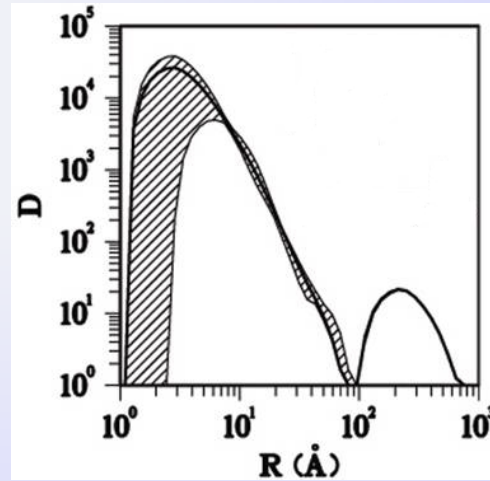
SANS cross-sections of implanted and reference samples

best-fit He bubble volume distributions  $D(R)$  ( $N(R) \times V(R)$ ) in  $\text{\AA}^{-1}$  in compared with the corresponding TEM histogram

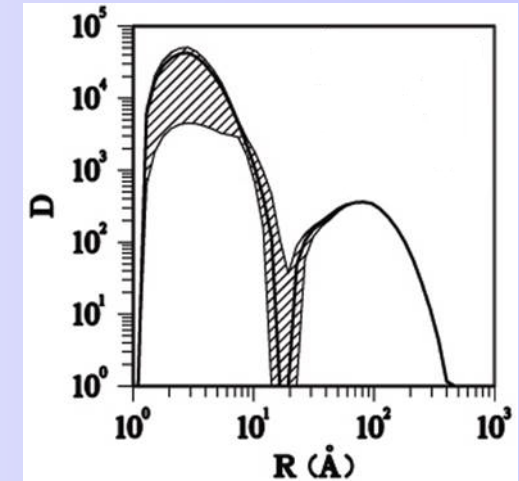
## Helium bubbles volume distribution in F82H-mod.



250 °C



825 °C

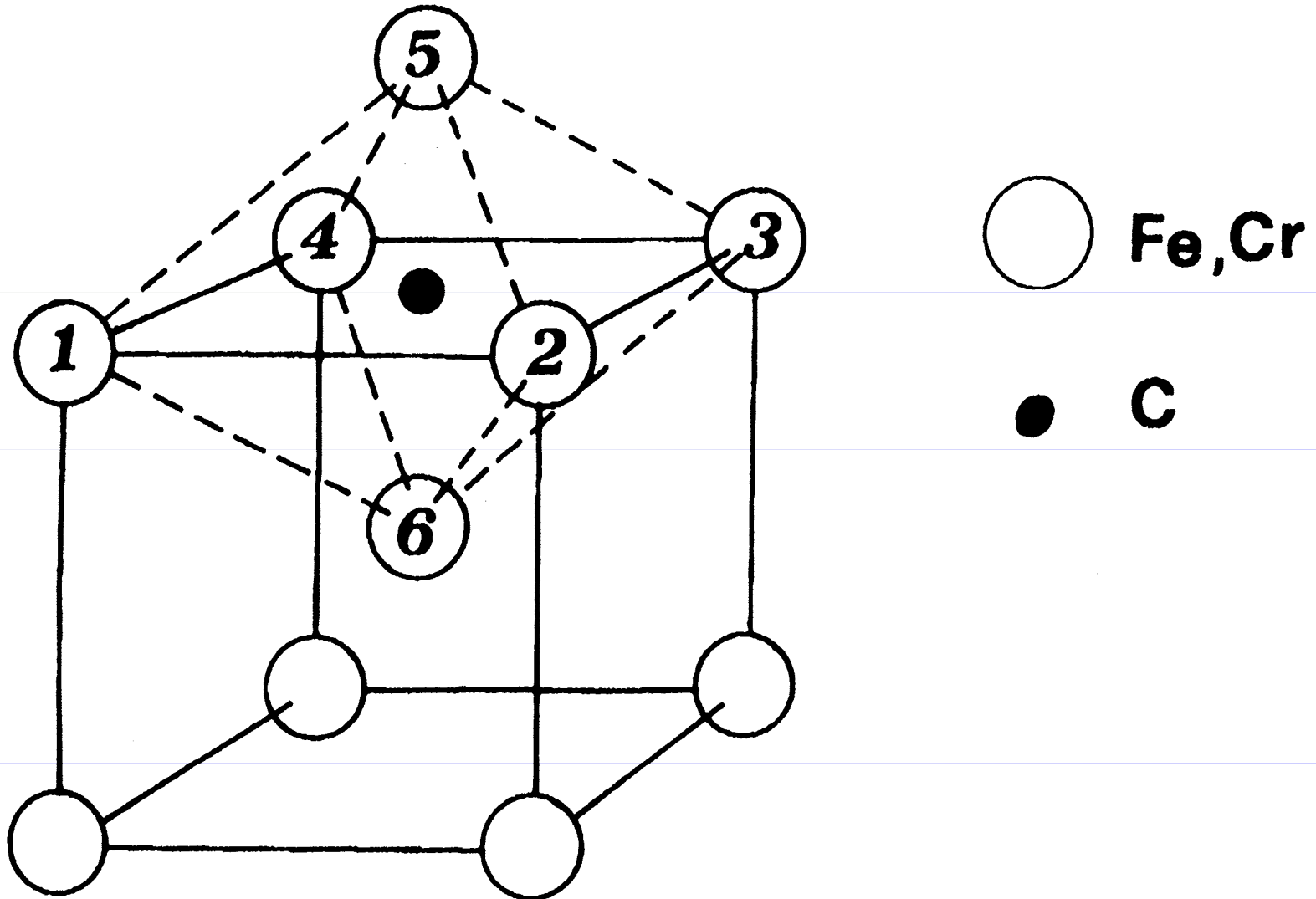


975 °C

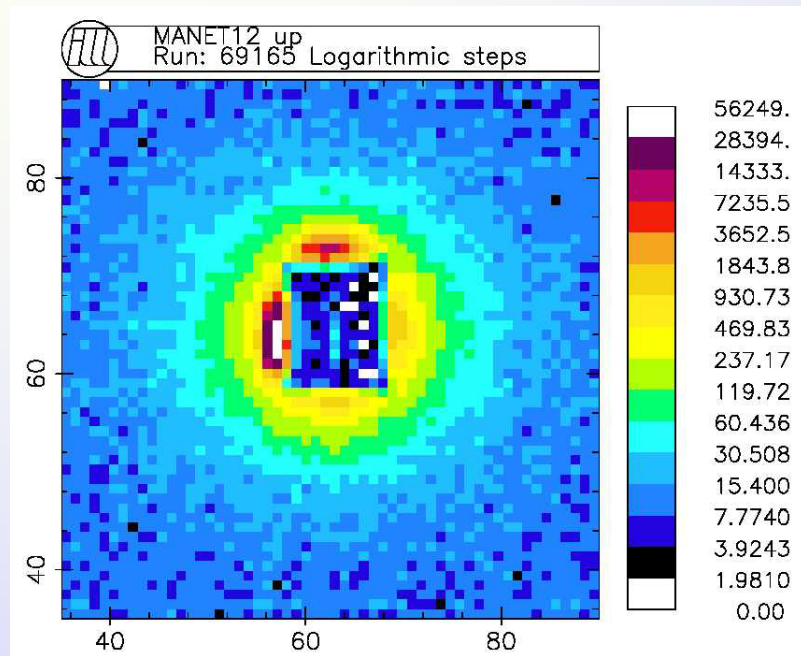
The dashed area represents the 80% confidence band

Best-fit helium bubble volume fraction,  $\Delta V$ , helium concentration,  $C_{He}$ , and radii obtained from SANS data. The  $R$  and  $\Delta V$  values in parentheses are those obtained from TEM.

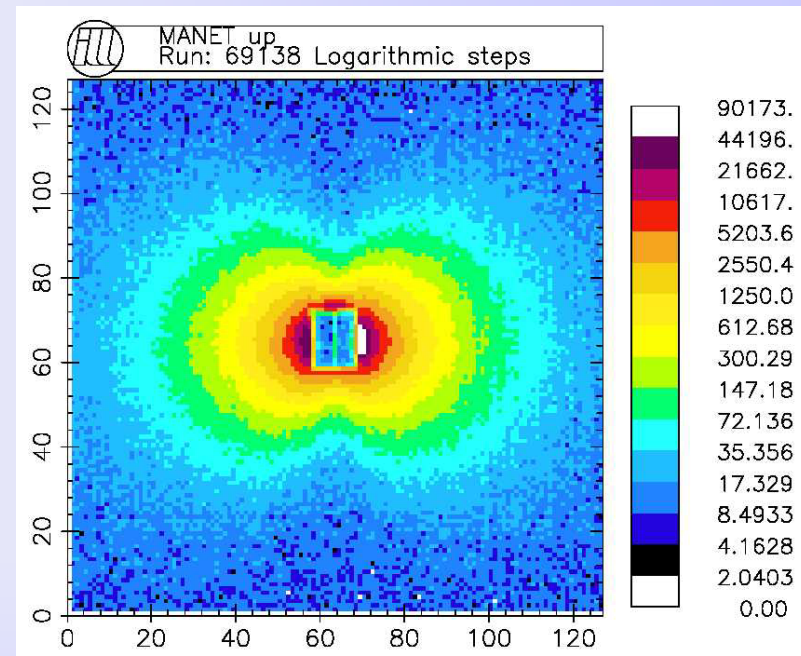
Tempering Temperature	$\Delta V$	$C_{He}(\text{appm})$	$R_V(\text{\AA})$
250 °C	0.0012 (0.0039)	209.0	11.1 (7)
825 °C	0.0053 (0.0036)	375.9	3.8 14.6 (17)
975 °C	0.0085 (0.0054)	558.9	4.1 45.9 (46)



The bcc lattice cell of MANET steel with an interstitial C atom in octahedral position; the six nearest neighbours can be Fe atoms or a number of Cr ones varying between 1 and 6 for the different thermal treatments

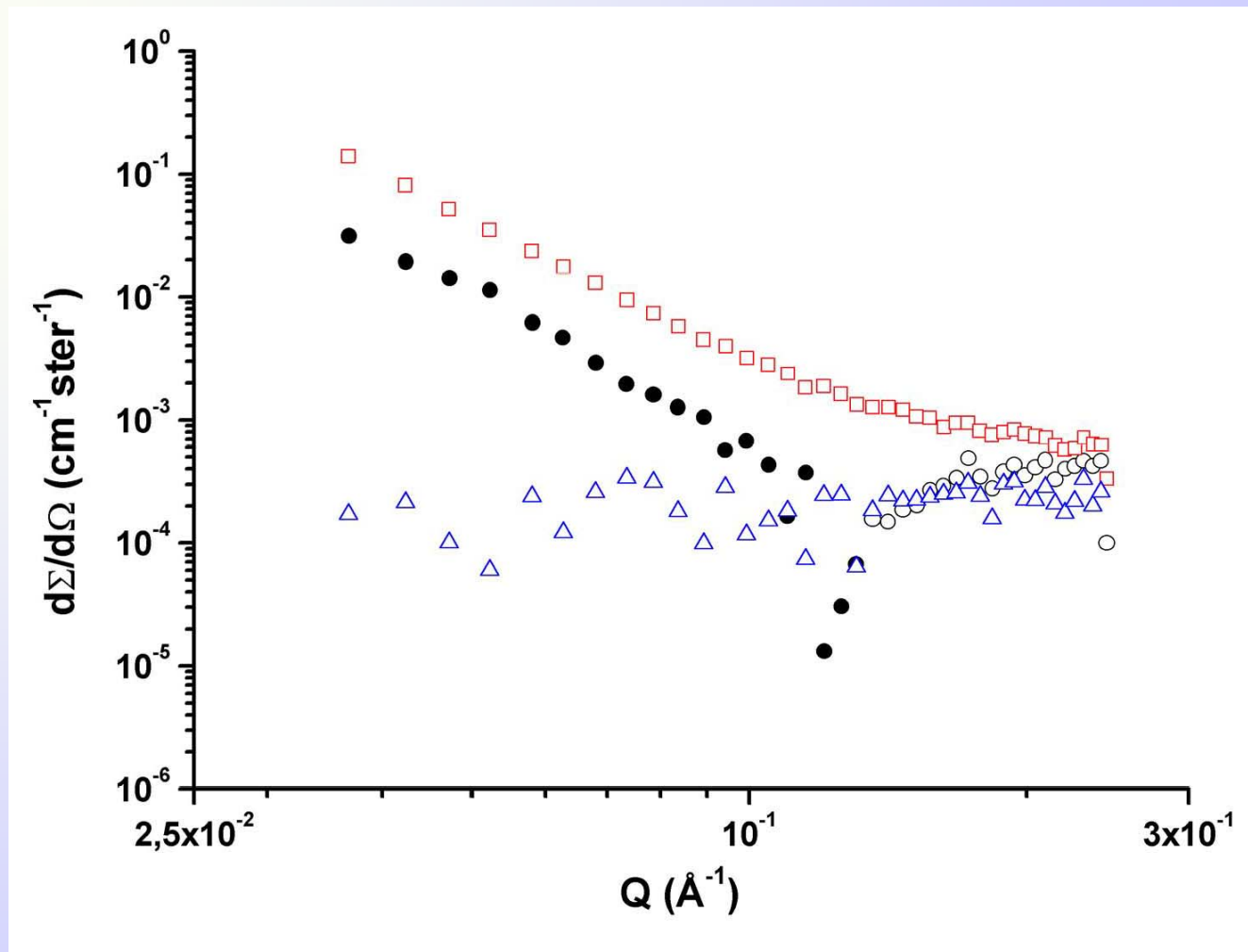


quench from 1200°



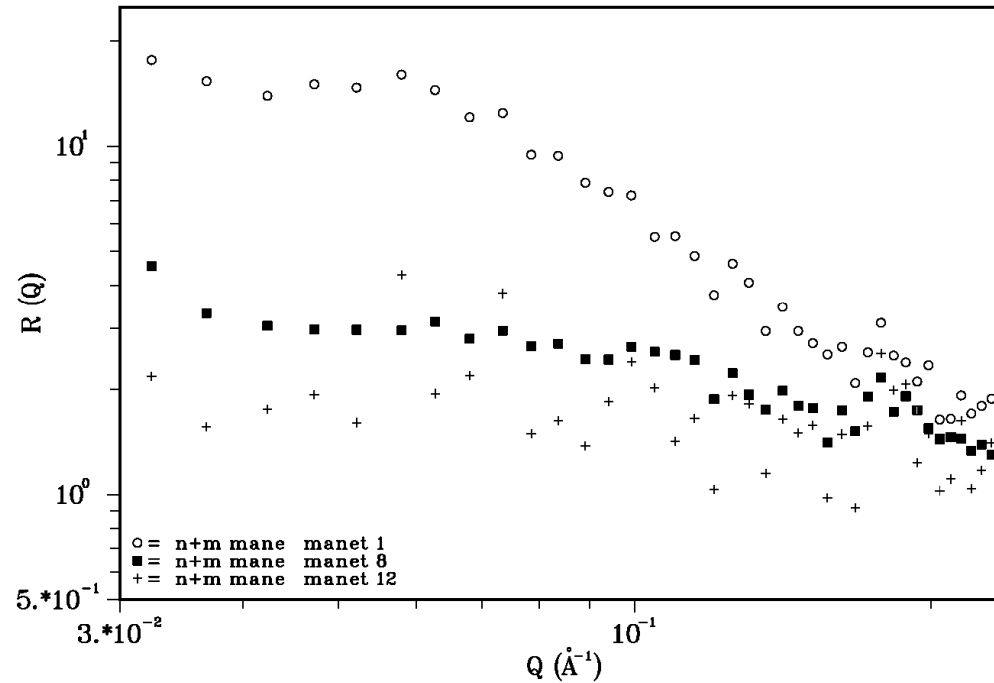
quench from 1075 °C

**The C-Cr elementary aggregates, giving rise to the magnetic anisotropy, dissolve for  $T > 1180^{\circ}\text{C}$**

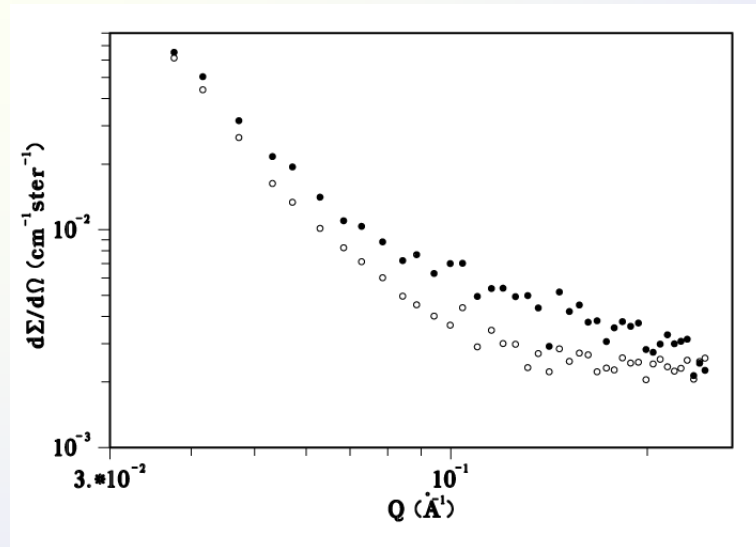


Nuclear-magnetic interference term for MANET quenched from **1075°C** (full dots moduli of the measured negative values, empty dots positive values), quenched from **1200°C** (triangles), quenched from 1075°C then **tempered 2 h at 700°C** (squares).

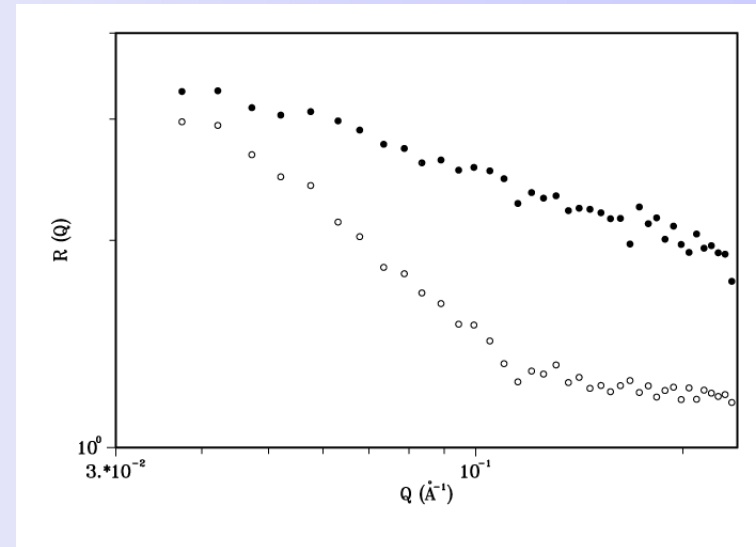
r manet1 manet8 manet12



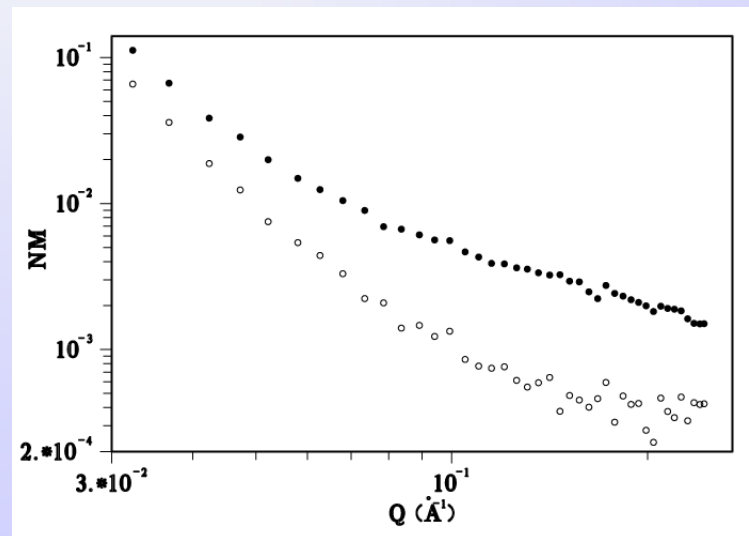
**R(Q) for MANET quenched from 1075°C (dots),  
quenched from 1200°C (crosses), quenched from  
1075°C then tempered 2 h at 700°C (squares)**



a )



b)



c)

(a) nuclear SANS cross-section  $N^2$  for reference (empty dots) and as-irradiated (full dots) MANET samples; (b)  $R(Q)$  ratio for reference (empty dots) and as-irradiated (full dots) MANET samples; (c) nuclear-magnetic interference term for reference (empty dots) and **as-irradiated at 250°C 0.8 dpa** (full dots) **MANET**.

# IRRADIATED MANET

**As-irradiated:** increase in N, R(Q) and NM with respect to reference

→ small magnetic defects ( $\alpha'$  precipitates)

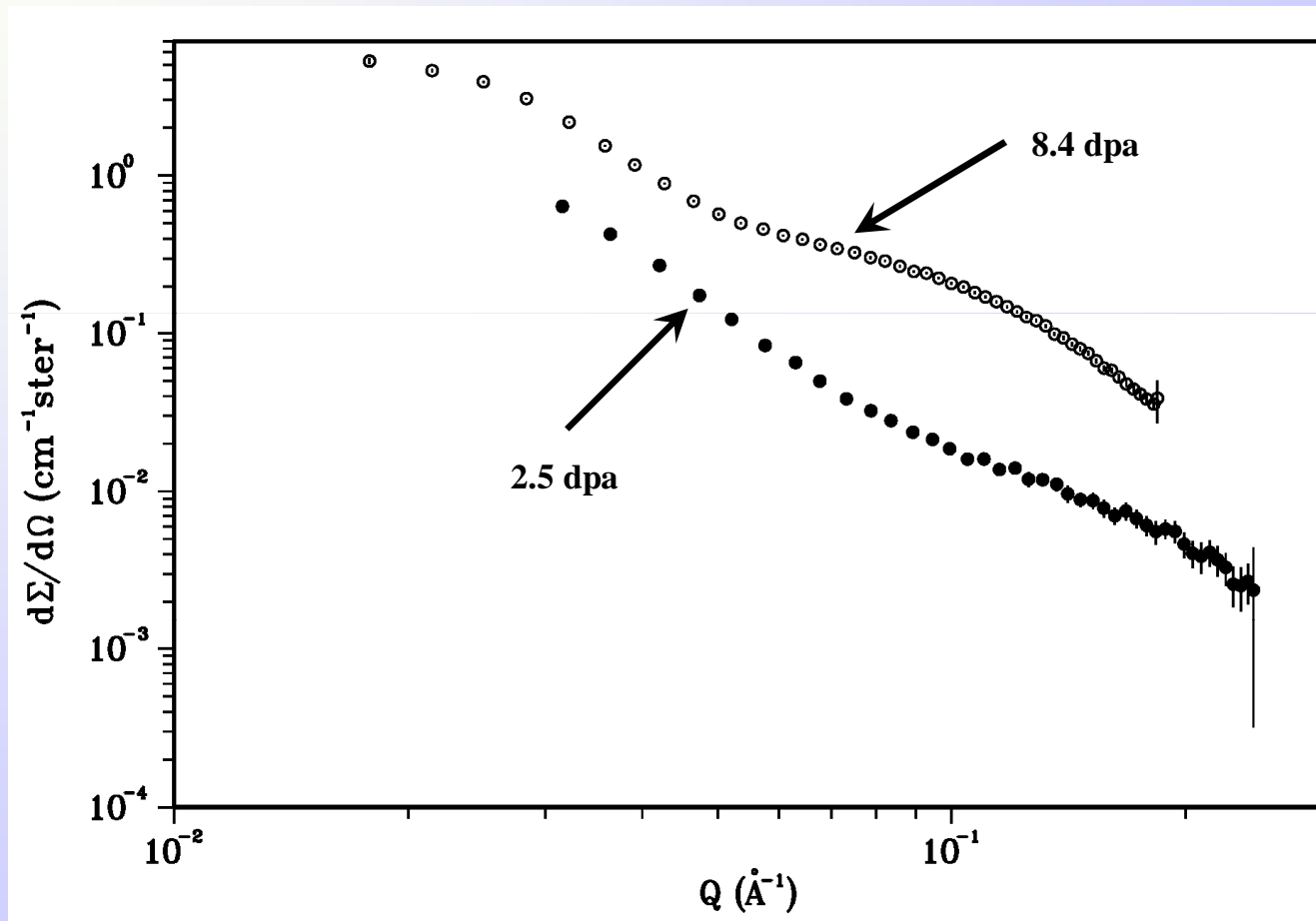
**Irradiated and tempered:** increase in N, no change in R(Q) and NM with respect to reference

→ large non-magnetic defects (microvoids, He-bubbles)

*Post irradiation tempering seems to promote the growth of large (1-10 nm) non-magnetic defects, such as He-bubbles or microvoids.*

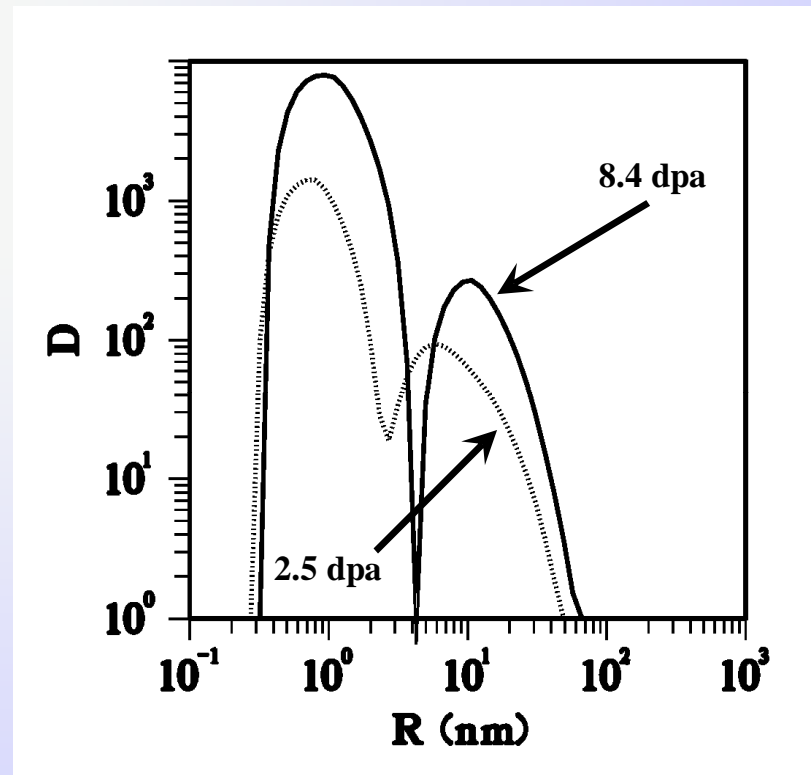
*This effect has been observed in other irradiated steels (data analysis underway).*

# RESULTS ON 2.5 AND 8.4 dpa IRRADIATED EUROFER (ICFRM13 Proceedings)



Nuclear SANS cross-sections of the difference between Eurofer97 neutron irradiated at 250°C at **2.5 dpa** and at 300°C at **8.4 dpa** and their respective reference samples

## MICROVOIDS EVOLUTION WITH IRRADIATION DOSE



Volume distribution functions  $D(R)$  ( $\text{nm}^{-1}$ ) obtained from the nuclear SANS difference between Eurofer97 neutron irradiated at  $300^\circ\text{C}$  and their respective reference samples

*Increasing the dose the average radius remains nearly unchanged but a consistent increase is observed in the volume fraction of the observed defects, from 0.005 at 2.5 dpa to 0.011 at 8.4 dpa*

## **WORK IN PROGRESS**

**refining the determination of the size distributions, for modeling purposes, with special attention to the effect of background subtraction**

**SANS measurements on B-doped Eurofer steel with up to 5000 He appm**

***in-situ* high temperature measurements for kinetics studies in Eurofer-ODS**

**TEM observation of irradiated Eurofer already investigated by SANS**

## REFERENCES

R. Coppola, C. Dewhurst, R. Lindau, R.P. May, A. Möslang, M. Valli, *Polarised SANS study of microstructural evolution under neutron irradiation in a martensitic steel for fusion reactor*, Physica B 345 (2004) 225

R. Coppola, M. Klimiankou, R. Lindau, R. P. May, M. Valli, *SANS and TEM study of  $Y_2O_3$  particle distributions in ODS EUROFER martensitic steel for fusion reactor* Physica B 350 (2004) 545

R. Coppola, M. Klimiankou, R. Lindau, A. Möslang, M. Valli, *Helium-bubble evolution in F82H mod – Correlation between SANS and TEM*, J. N. M. 329-333 (2004) 1057

R. Coppola, R. Lindau, M. Magnani, r. P. May, A. Möslang, J. W. Rensman, B. van der Schaaf, M. Valli, *Microstructural investigation, using SANS, of neutron irradiated Eurofer97 steel*, F. Eng. & Des. 75-79 (2005) 985

R. Coppola, R. Lindau, R. P. May, A. Möslang, M. Valli, *Investigation of microstructural evolution under neutron irradiation in Eurofer97 steel by means of small-angle neutron scattering*, J. Nucl. Mat. 386-388 (2009) 195-198

R. Coppola, R. Lindau, R. P. May, A. Möslang, M. Valli, P. Vladimirov, A. Wiedenmann, *SANS study of microstructural evolution in oxide strengthened EUROFER steel after heat treatments*, pres. at ICNS2009 and sub. J. Phys. C